Short Polyaniline Nanorod Prepared in the Presence of *para*-Phenylenediamine

Liang Chao,[1] Ko-Shan Ho,[2] Sheng-Yen Shen,[2] Hsin-Yu Pu,[2] Tar-Hwa Hsieh,[2] Chung-Wen Kuo,[2] Bo-Hao Tseng[3]

[1]Center for General Education, Taipei Chengshih University of Science and Technology, Peito, Taipei 11202, Taiwan
[2]Department of Chemical and Materials Engineering, National Kaohsiung University of Applied Sciences, Kaohsiung 807, Taiwan
[3]Department of Optics and Photonics, National Central University, Jhongli City, Taoyuan County 32001, Taiwan

Correspondence to: K.-S. Ho (E-mail: hks@cc.kuas.edu.tw)

ABSTRACT: *para*-Phenylenediamines (pPDAs) were mixed with aniline to synthesize a low molecular weight, nanowired polyaniline via emulsion polymerization, which demonstrated smaller intrinsic viscosity. Fourier transform infrared-spectra illustrated the presence of phenazines in the polymers in the presence of pPDA. Free carrier-tails in UV-Vis-NIR spectra are still present but their numbers decreased with pPDAs. Scanning electronic microscopy and transmission electronic microscopy (TEM) images showed the neat PANINTs shrank significantly and became randomly distributed after dedoping but the diameters of the PANINT-pPDAs decreased slightly. TEM micrographs demonstrated the hollow morphology for the neat PANINTs but that of PANINT-pPDA was shorter, solid nanowires. X-ray diffractions patterns illustrated a layered structure for neat PANINTs which own a long c-axis, not found for PANINT-pPDAs. © 2012 Wiley Periodicals, Inc. J. Appl. Polym. Sci. 000: 000–000, 2012

INTRODUCTION

In recent years, polyaniline nanostructure has been widely studied. Nanotubular polyanilines can be prepared from the chemical oxidative polymerization approaches including the use of insoluble solid templates such as zeolites,[1] opals,[2] controlled pore-size membranes,[3] and anodic aluminum oxide[4] or soluble templates such as polymers[5] and surfactants.[6] When organic, protonic acid dopants with long hydrophobic tails are used as surfactants, emulsified micelles can be formed leading to micro-tubes, -fibers, or -rodlike morphologies[7–11] due to the self-assembled effects. The polyaniline molecules inside of the micro- or nano-rods need to be extended to fit into the long nanorod-like polymers. Therefore, the end-to-end distance of the polyaniline molecules inside of mico- or nano-tubes or rods should be much higher compared with the common polyaniline ones which own conformations close to worm-like or random-coil model, especially when their molecule weights are high enough and can be considered still as random-coil like molecules. Consequently, the molecule weight of a polymer molecule which can be fit into a tubular or rod-like frame should not be too long and cannot adopt the so-called random-coil conformation.

In our previous studies,[12,13] we were able to prepare a hollow, nano-polyaniline tube (PANINT) in a facile way by reducing its molecule weight through shortening the emulsion polymerization time in the presence of *n*-dodecylbenzenesulfonic acid (DBSA) and mineral hydrochloric acid. Besides, we found that PANINT can absorb almost whole range of NIR, which is usually found for inorganic materials like indium tin oxide (ITO), antimony tin oxide (ATO) particles. Therefore, it is possible to apply this organic, common solvent (toluene and xylene) soluble PANINT as the printable IR-absorber which can be easily coated on the transparent film and become sun-heat blocker that can be put on the glass panels of cars or windows.

para-Phenylenediamine (pPDA) was proved to be able to reduce the molecular weight of polyaniline[14–21] effectively and was often chosen as the inhibitors for polyaniline polymerization. We are going to see what can happen to the IR blocking capability of the PANINT when its molecular weight (MW) is decreased by the presence of pPDA through the following studies.

EXPERIMENTAL

Materials

The aniline monomer (Tokyo Kasei Kogyo Co.) was distilled under vacuum before use. Ammonium persulfate (APS, Showa

Chemicals Instrument Co.), DBSA (Tokyo Kasei Kogyo Co.), and pPDA (Tokyo Chemical Industry Co.) were used without further purification.

Synthesis of Nanotubular Polyanilines with and without pPDA

In this experiment, micelles were formed after the addition of 0.052 mol of DBSA in 50 mL of water with vigorous magnetic stirring. Then, 0.13 mol aniline monomer and 1%, 3%, and 5% of pPDA in molar ratio was introduced, respectively, followed by magnetic stirring for 10–15 min and some phosphoric acid was added to reduce the pH value until it is below one. A 0.01 mol APS was dissolved in 30 mL of water and was poured onto the monomer solution with vigorous stirring at room temperature. After about 1 h, the mixture was filtered to obtain the filter cake, which was then washed with acetone until the filtrate became colorless. The cake was then dried at 60° for 24 h in a

Table I. Intrinsic Viscosity and MW of EB Type PANINTs

	$[\eta]^a$	$M_v{}^b$
EB of neat PANINT	3.341	27,400
EB of PANINT-pPDA-1	0.778	13,100
EB of PANINT-pPDA-3	0.705	12,200
EB of PANINT-pPDA-5	0.611	11,000

[a]The intrinsic viscosity was calculated from the below equation[22] $[\eta] = \frac{1}{c} \cdot \sqrt{2} \cdot (\eta_{sp} - \ln \eta_r)$, [b]$M_v$ was calculated from the Mark-Houwink relation of polyaniline in NMP at 30°C[23]: $[\eta] = 1.95 \times 10^{-6} M_v{}^{1.36}$.

vacuum oven. The obtained products were named as PANINT-pPDA-1, 3, and 5, respectively.

A comparison experiment in the absence of pPDA was carried out with the same polymerization conditions except the shorter polymerization time (30 min) and the obtained product is named as neat PANINTs.
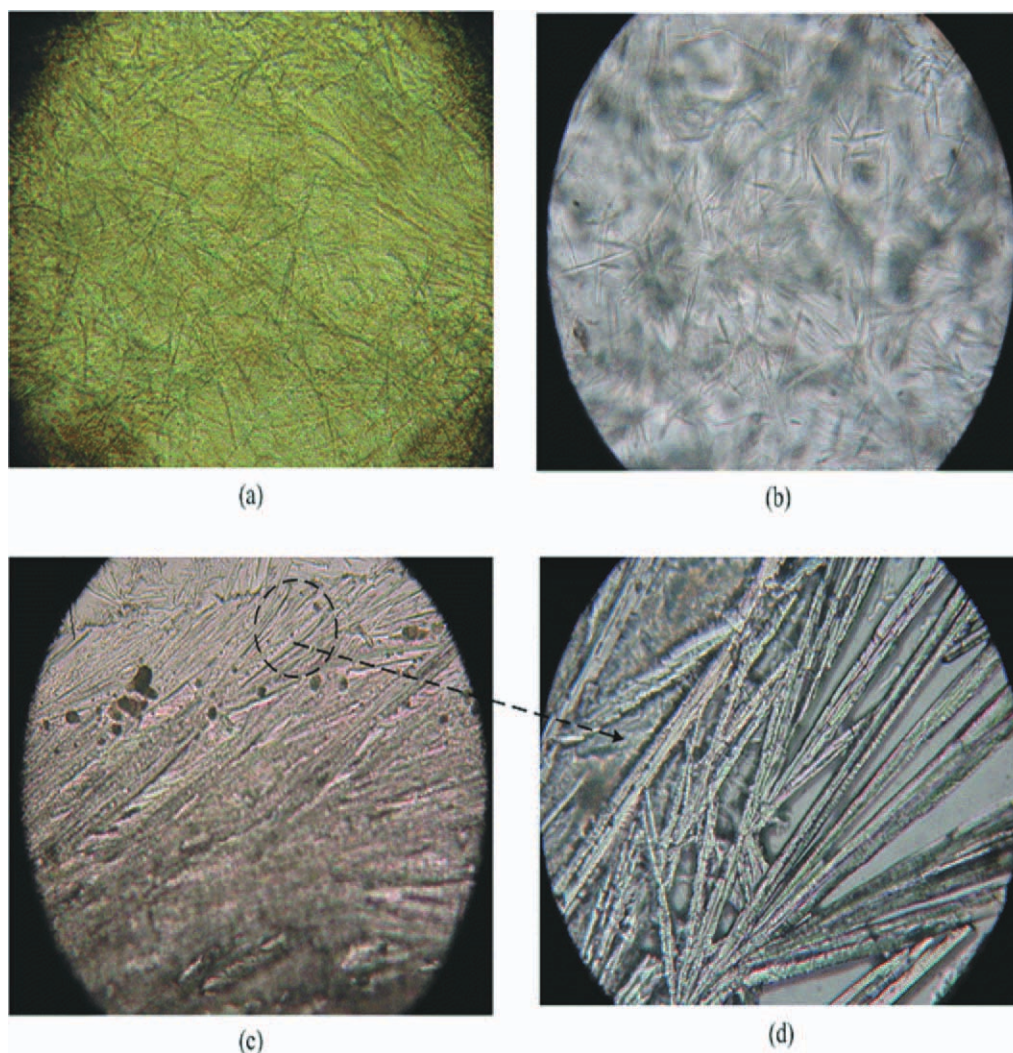

Figure 1. Optical pictures with 100 magnifications of (a) DBSA + Water + aniline, (b) DBSA + Water + aniline + 5% pPDA, (c) DBSA + Water + aniline + 5% pPDA + H$_3$PO$_{4(aq)}$, and (d) scaled up picture of (c) with 400 magnifications. [Color figure can be viewed in the online issue, which is available at wileyonlinelibrary.com.]
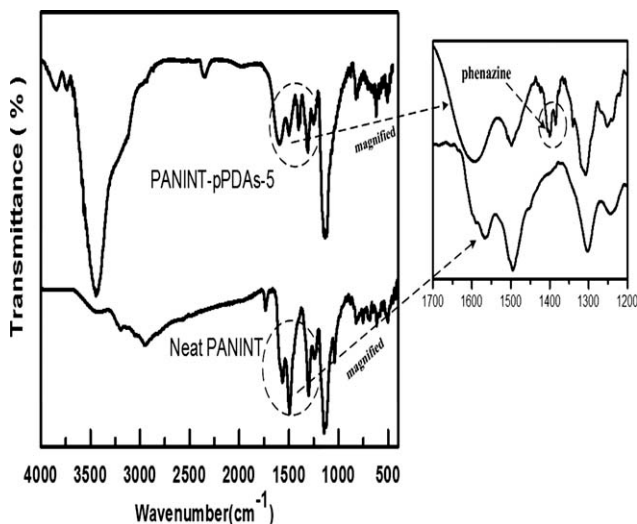
Figure 2. FTIR spectra of neat PANINT and PANINT-pPDA-5.

All PANINTs were dedoped into emeraldine base (EB)-types by mxing with $1M$ ammonium water, stirring overnight, followed by drying in vacuum oven for at least 24 h.

An EB type of tetraaniline was prepared by oxidizing p-phenyl-p-phenylenediamine with ferric chloride in HCl (aq) followed by dedoping in $1M$ ammonium water overnight.

Tetraanilines were prepared from ferric chloride and pPDA, which were dissolved in 100 mL and 500 mL $0.1M$ hydrochloric acid, respectively. The ferric chloride solution was added to the pPDA suspension with vigorous stirring for 2 h because the mixture became very sticky easily. After 2 h, tetraaniline doped with hydrochloric acid was obtained and separated by centrifugation. The EB type tetraaniline was obtained after washing with $0.1M$ ammonium hydroxide for 2 h and collected by vacuum filtration and dried in oven at $60°C$ for more than 24 h.

Characterization
Polarized Optical Microscopy. Emulsified monomers solution was cast on a microscope glass plate ($7.6 \times 2.54 \times 0.1$ cm^3) and covered with cover glass to prevent the evaporation of water and taken polarized optical pictures by an Olympus BH-2 optical microscope.

Intrinsic Viscosity ($[\eta]$) and Molecular Weight. The $[\eta]$ of EB types of various PANINTs were carried out in n-methylpyroli-done (NMP) solvent with Ubbelohde viscometer in a heating bath controlled at $30°C$. The $[\eta]$ value was calculated directly from the equation shown in Table I[22] and was used to calculate the MW according to the Mark-Houwink relation ($[\eta] = KM_v^a$) with $K= 1.95 \times 10^{-6}$ and "a" $= 1.36$ in NMP.[23]

IR Spectroscopy. The functional groups of the neat PANINTs and PANINT-pPDA-5 were characterized by Fourier transform infrared (FTIR) spectroscopy. The FTIR spectra were recorded
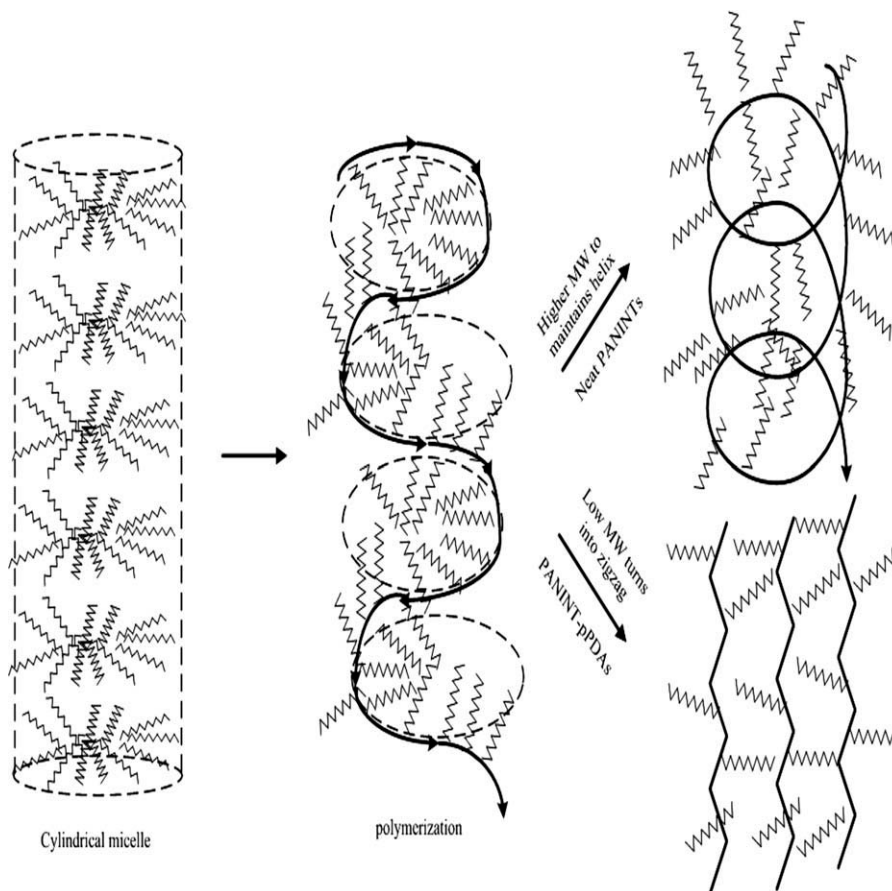
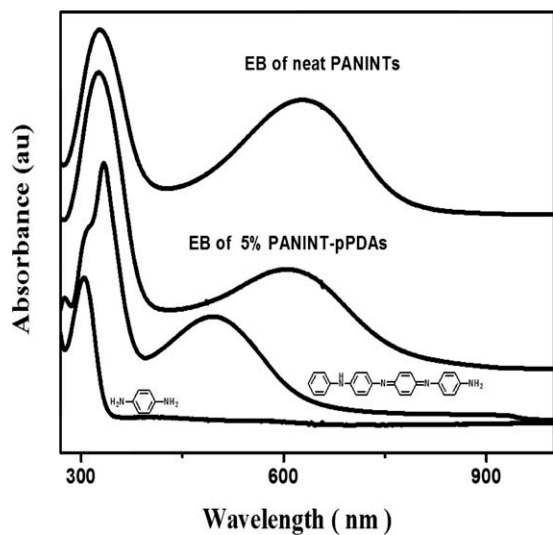**Scheme 1.** Formation mechanism of phenazine in the presence of pPDA.

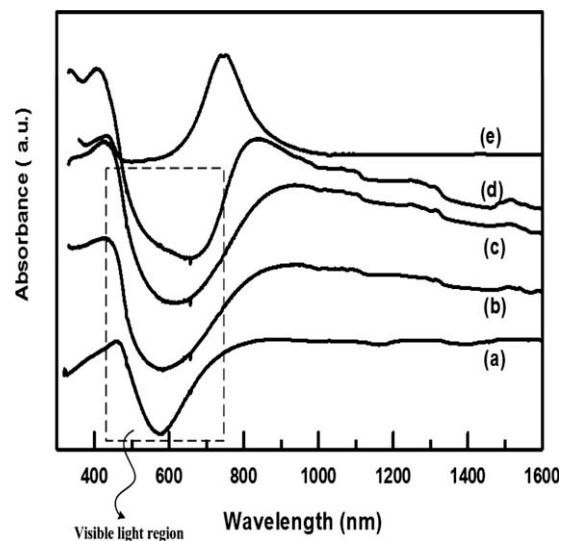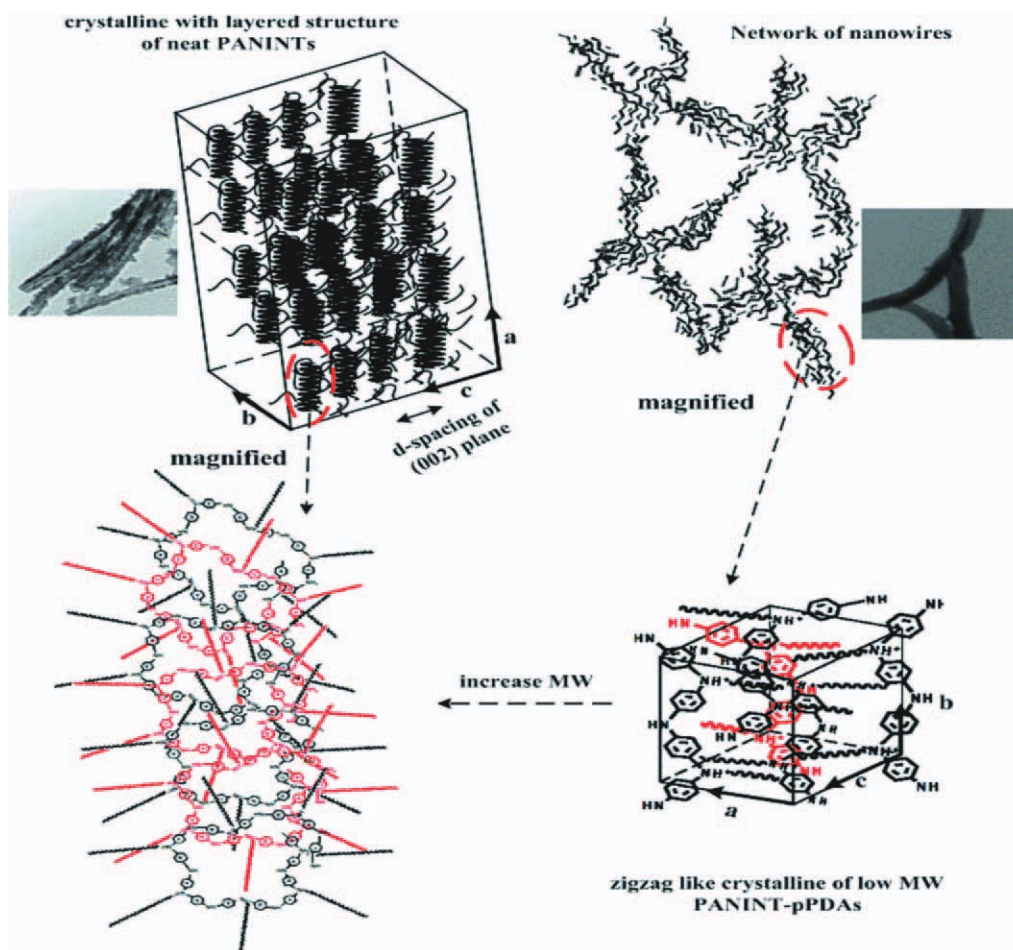**Figure 3.** UV-Vis-NIR spectra of PPDA, EB-types of tetraaniline, and PANINTs.

Figure 4. UV-Vis-NIR spectra of (a) neat PANINTs, (b) PANINT-pPDA-1, (c) PANINT-pPDA-3, (d) PANINT-pPDA-5, and (e) PANIDBSA.

Scheme 2. Conformational change during polymerization for various PANINTs. [Color figure can be viewed in the online issue, which is available at wileyonlinelibrary.com.]
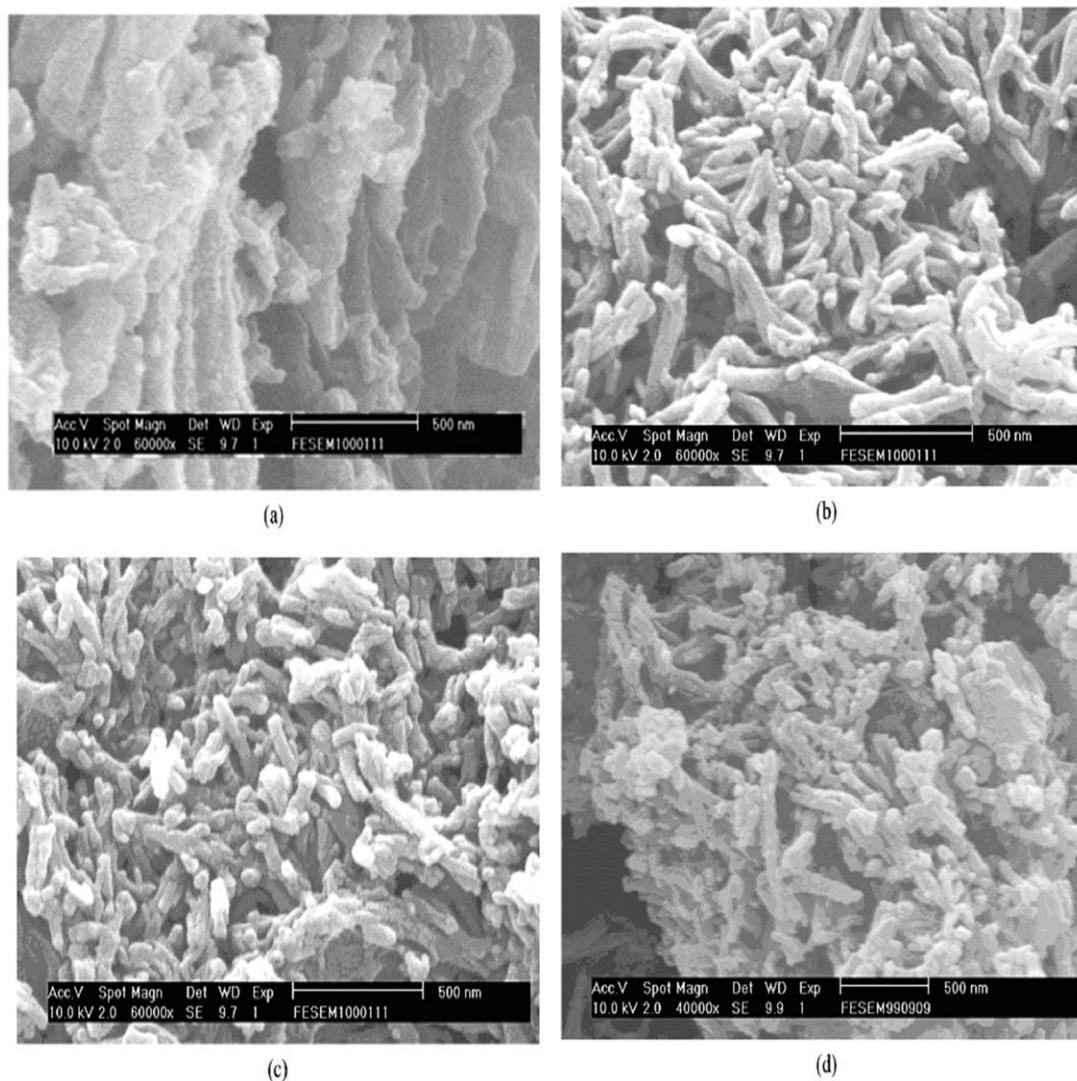
Figure 5. SEM micrographs of various PANINTs: (a) neat PANINTs, (b) PANINT-pPDA-1, (c) PANINT-pPDA-3, and (d) PANINT-pPDA-5.

on an IFS3000 v/s Fourier transform infrared spectrometer at room temperature.

UV–Vis-NIR Spectroscopy. The UV-Vis-NIR spectra of the samples were obtained from a Hitachi U-2001 and DTS-1700 NIR Spectrometer. The wavelength ranged from 300 to 1600 nm.

Scanning Electronic Microscopy (SEM). Images of PANINTs were taken in a Field Emission SEM, HRSEM (HITACHI S-4200: accelerating voltage of 15 kV) prepared from strewn on carbonic tape and followed by posting on ferric stage.

Transmission Electronic Microscopy (TEM). Samples for field emission transmission electron microscope, HR-AEM (HITA-CHI FE-2000) were first dispersed in acetone and put on carbonic-coated copper grids in drop wise before subjected to the emission.

Wide Angled X-Ray Diffraction (WAXD). An copper target (Cu-K$_\alpha$) Rigaku x-ray source with a wavelength of 1.5402 Å was

used for diffraction. The scanning was performed with a voltage of 40 kV and a current of 30 mA at a scanning rate of 1°/min.

RESULTS AND DISCUSSION

Polarized Optical Microscopy

The monomer mixtures before the addition of APS initiator were taken optical pictures to illustrate the aggregation of the self-assembled anilinium monomers with or without pPDA. When aniline monomers were complexed with DBSA counter ions (anilinium DBSA salts), they were able to self-assemble into separated cylindrical micelles,[24,25] which can be clearly seen by the optical microscopic picture shown in Figure 1(a). The introduction of pPDA, as seen in Figure 1(b), rendered the monomer mixtures to become stiff, short rods which were aligned into bundles when phosphoric acids were added as shown in Figure 1(c,d). It is understood that polyacids like H_3PO_4(aq) are able to complex with two amino-groups from different cylindrical micelles and to link them together through the pPDA bridges (DBSA$^-$+H$_3$N—⟨⟩—NH$_3^+$ $\cdot$ $^-$PO$_4$H$^+$NH$_3$—⟨⟩—NH$_3$$^{+\cdot}$ DBSA).
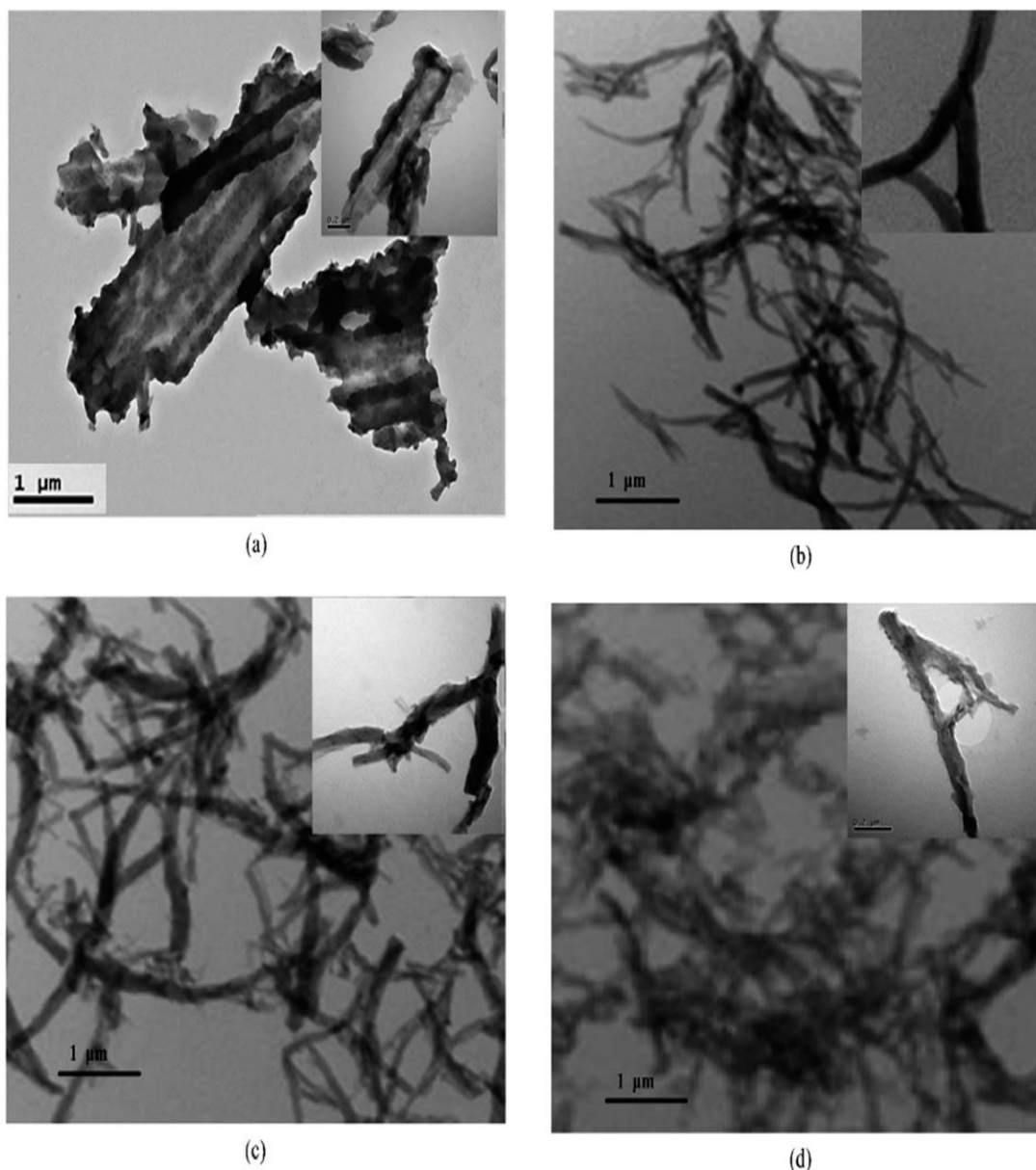
Figure 6. TEM micrographs of various PANINTs: (a) neat PANINTs, (b) PANINT-pPDA-1, (c) PANINT-pPDA-3 (d) PANINT-pPDA-5, all inset images are locally magnified views.

Molecular Weight Measured by Viscometer

Common MWs of polymers are measured by gel permeation chromotography (GPC) which assumes all molecules are spherical, random-coiled because the packing materials inside GPC column own lots of spherical pores on their surfaces. Therefore, rod-like polyanilines, which are not in the spherical form will not easily to fit into the spherical pores of GPC and the obtained MWs, are usually overestimated, depending on their shapes. In this study, we measured intrinsic viscosity of different types of PANINTs at constant temperature to calculate the viscosity-averaged MW with Mark-Houwink relation which has an order equal to 1.36, higher than the maximum value of 0.8 for random-coil polymers shown in Table I.[22] The polyanilines were first dedoped by ammonium water overnight to remove all protonic acids to become EB (emeraldine base) type before dissolv-

ing in NMP solvents. The obtained intrinsic viscosities were listed in Table I and converted into viscosity-averaged MW (M_v).[23] The M_v turned out to be about 11,000 and 27,400 g/mol for EB types of PANINT-pPDA-5 and neat PANINT, respectively, listed in Table I. The presence of some pPDA (1%, 3%, and 5%) can effectively decrease the MW of PANINTs to about one-half.

FTIR Spectroscopy

Based on the chemical structure for PANINT-pPDA, the only possible difference when PANINTs were prepared in the presence of 5% pPDA is the double number of amino-chain ends. One can obtain a PANINT with two amino-chain ends which were usually used to condensate with other functional monomers to become a blocked copolymer with polyaniline.[26]
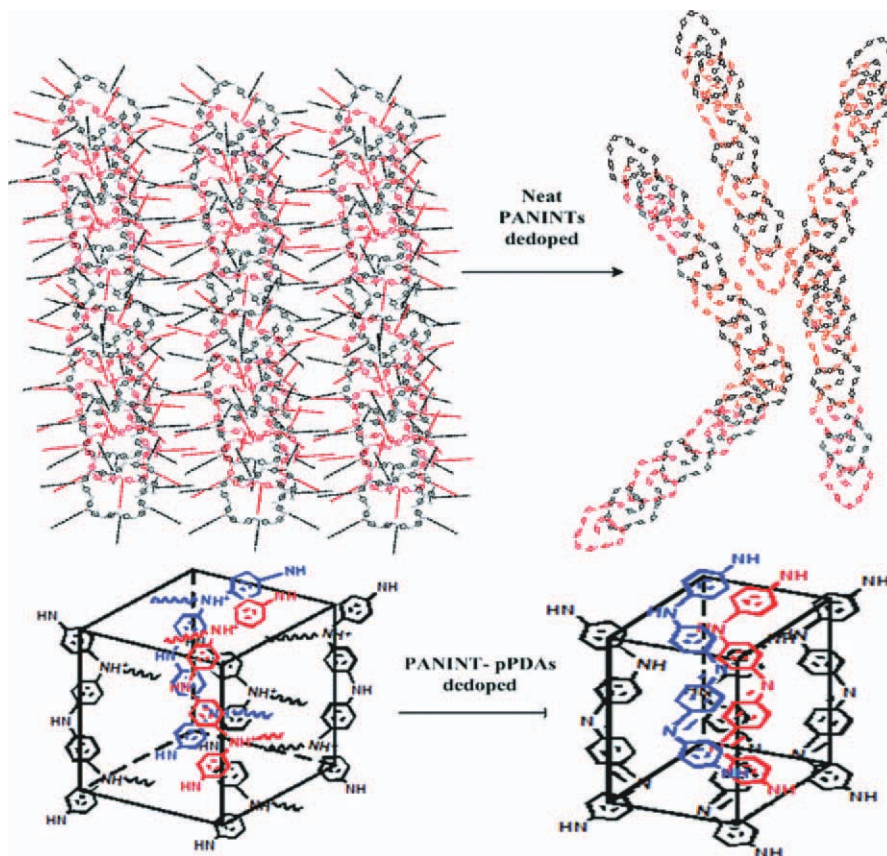
Scheme 3. Hollow nanotubes and solid nanowires of various PANINTs. [Color figure can be viewed in the online issue, which is available at wileyonlinelibrary.com.]

Based on the FTIR spectra illustrated in the inset of Figure 2, the traditional absorption peaks for benzenoid 1496 cm^{-1} can be found for both neat PANINT and PANINT-pPDA-5. However, the quinoid peak of PANINT-pPDA-5 appeared at higher wavenumbers when compared with that of neat PANINT, indicating the presence of different degree of doping for PANINT-pPDA-5.

Additional peak around 1400 cm^{-1} was found for PANINT-pPDA-5 due to the presence of phenazine which can be obtained from the combination of radicals of anilinium and pPDA at the ortho-position[27] because the para-position of pPDA has been occupied by the other amine. The possible phenazine formation mechanism is demonstrated in Scheme 1.

UV–Vis-NIR Spectroscopy

Through the UV-Vis-NIR spectra of pPDA and tetraanilines in Figure 3, we understand that the charge transfer from the benzenoid to quinoid rings can contribute to the λ_{max} at the higher wavelength in the visible or near-IR region. In Figure 3, no λ_{max} at visible or NIR region can be found for neat pPDA due to the absence of quinoid ring. However, additional peak at high wavelength started to appear if the quinoid ring was present on the backbones of EB types of tetraaniline and polyanilines. When the MWs increase, we can see the red-shift of the transition from benzenoid to quinoid rings. There is already a λ_{max} at
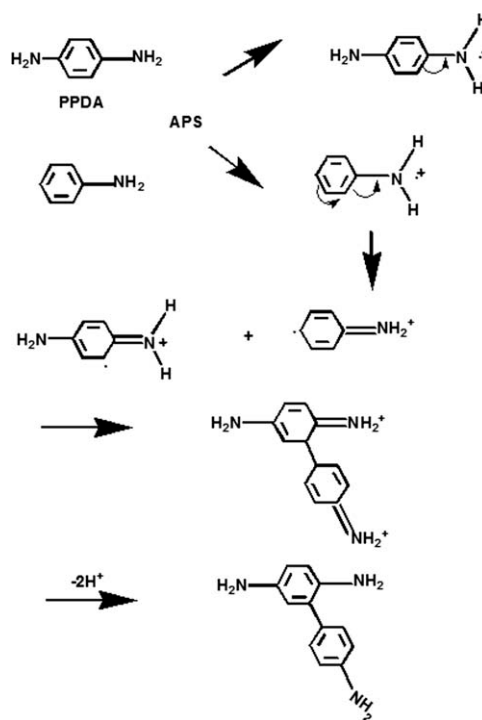
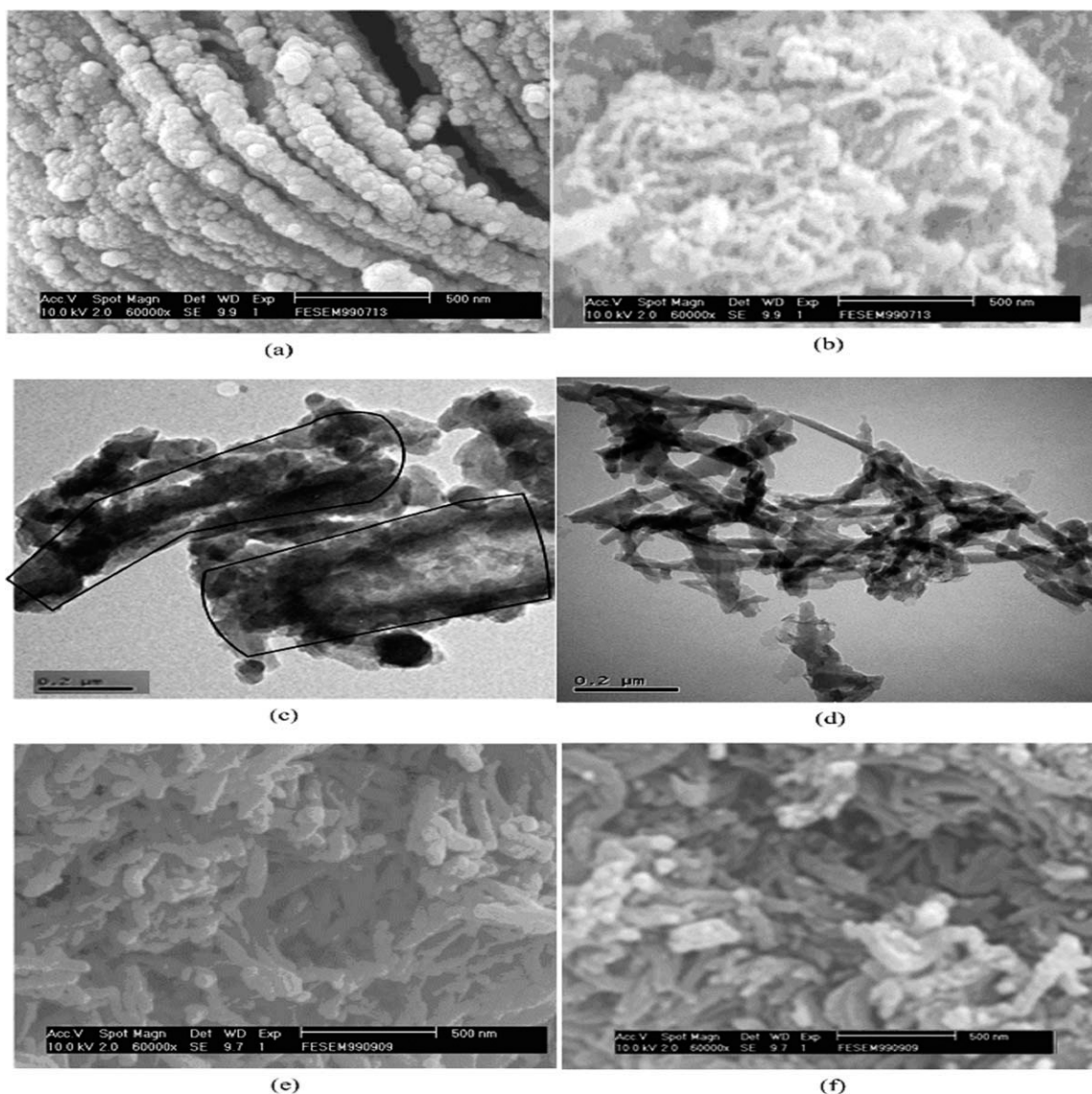**Scheme 4.** Branch formation mechanism of PANINT-pPDAs.

Figure 7. SEM micrographs of (a) ES-type (b) EB-type and TEM micrographs of (c) ES-type (d) EB-type of neat PANINTs and SEM micrographs of (e) ES-type and (f) EB-type of PANINT-pPDA-1.

around 500 nm, pretty close to that of EB type of PANINT-pPDA-5s (605 nm) or neat PANINTs (655 nm), which has more than 300 aniline units (M_v = 27,400 and MW of aniline = 92 g/mol). The λ_{max} difference between tetraaniline and PANINT-pPDA-5 is around 95 nm with more than 150 monomer unit difference. The difference of numbers of polymerized aniline units between PANINT-pPDA-5 (M_v = 11,000 g/mol) and neat PANINT is about 190. However, the λ_{max} difference between them is just 50 nm. Therefore, we can understand the PANINT-pPDA-5 molecule has a straighter conformation than that of neat PANINT. Clearly, the λ_{max}, which is related to the benzoid to quinoid transition, does not proportionally red-shifted with MW.

The ES (emeraldine salt) type of polyanilines can be well-dispersed in the toluene solvent if the protonic acid dopants own long alkyl chains. In that case, their UV-Vis spectra can be obtained in the toluene. For nontubular polyanilines like PAN-IDBSA which was prepared with DBSA as the only protonic acid, the λ_{max} was at around 780 nm and did not demonstrate any free carrier-tail at the visible or NIR region as shown in Figure 4(e). The absorption at these regions is considered as the capability to absorb the hot NIR from the sunlight. For tubular polyaniline, free carrier-tail absorption at the NIR range has made it possible as one of the few organic candidates that can be used to block the hot NIR radiation from the sunlight. For neat PANINTs which were prepared with short polymerization time in the presence of both long alkyl acid (DBSA) and mineral acids (H_3PO_4) demonstrates a nearly flat plateau of carrier-tails covering almost entire NIR region as shown in Figure 4(a), indicating PANINT molecules are in the highly conjugated state. To avoid the repulsion force (steric hindrance) between the intramolecular long benzenedodecyl chains of complexed DBSA

dopants and to accommodate these huge side chains, the possible conformation for the PANINTs molecules is to become nanotubes of coiled molecules which can exclude some complexed DBSAs outside (Scheme 2). The helically coiled conformation (not randomly coiled) can still retain the highly conjugated state and resulted in a hollow, tubular structure[12] with molecules winding and circulating along the cylinder with least interruption of conjugation and bending of the backbone. It also attributed to the significant free carrier-tail range found in the NIR region for neat PANINTs. However, it still has a strong absorption in the visible light region (like a V-shape at the visible region), which can largely decrease its transparency if it is wanted to be applied as a transparent IR cutting material that is oftenly seen as the heat-insulated film covered on the glass windows of cars.

Luckily, the absorption at the visible region can be depressed (U-shape at the visible region) when the length of the PANINT was shortened by decreasing its MW with the addition of pPDAs as shown in Figure 4(b–d). We also found that shoulder or peak at the NIR region gradually appeared and blue-shifted when more pPDAs were introduced, resulting from the decreasing MW and conjugation length of the PANINT-pPDAs compared with that of neat PANINTs. Both λ_{max} at UV (π to π^*) and at NIR regions blue-shifted with pPDA due to the shortening chains. The maximum wavelength absorptions (>800 nm) of PANINTs with or without pPDA are still higher than that of the nontubular PANIDBSA (780 nm).

SEM and TEM

The SEM micrograph in Figure 5(a) illustrates that neat PANINTs are made of long, well-aligned nanorods with diameters of about 200 nm. When its MW was reduced in the presence of pPDA, these nanorods became smaller, shorter, and were randomly oriented as shown in Figure 5(b–d). The diameters of these nanowires became smaller with pPDA. Because SEM micrographs cannot distinguish these 1D nanowires were solid or hollow, TEM micrographs were taken to check the wires were hollow or not.

Because of the smaller MW of PANINT-pPDAs, they displayed a solid nanowire network as seen in Figure 6 of TEM micrographs. The repulsion force developed from the neighboring side-chain like, long DBSAs and the shorter backbones of PANINT-pPDAs was not able to maintain a helix-like conformation. Eventually, the coiled chains are released and reconform into more compact, zigzagged conformation (Scheme 2). These zigzagged molecules are easy to crystallize into an orthorhombic lattice, leading to the formation of the solid nanowire seen from Figure 6(b–d) and sketched in Scheme 3. Therefore, in the presence of pPDA, the as-synthesized polyaniline molecules demonstrated the shorter, solid nanowires with no hollow space can be seen on their TEM micrographs. These nanowires are prone to form a network like morphology because pPDA can connect two nanowires that are sharing the same phosphoric acid molecule (^+H_3N—⟨⟩—NH_3^+ · PO_4H^+ NH_3⟨⟩—NH_3^+). The presence of pPDAs in the polymerization can also cause the formation of branched polymers by polymerizing at both ortho- and para-positions (Scheme 4). Besides, the nanowires of PANINT-pPDAs have
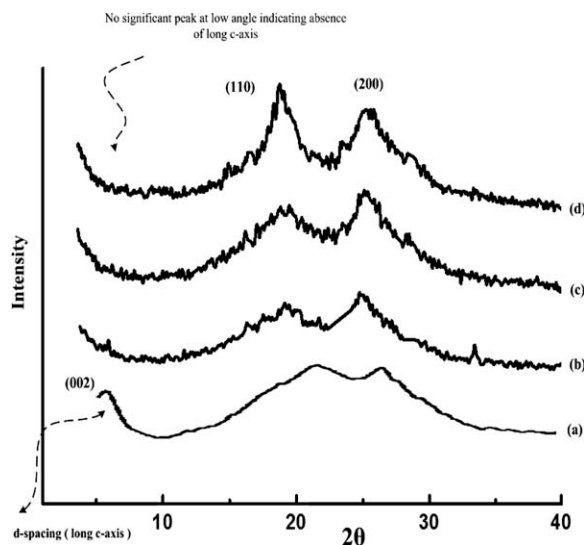

Figure 8. X-ray diffracton patterns of various PANINTs: (a) neat PANINTs, (b) PANINT-pPDA-1, (c) PANINT-pPDA-3, and (d) PANINT-pPDA-5.

smoother surfaces compared with that of neat PANINT, which owns rougher surface resulting from the more coiled conformations according to the inset images on the right, upper part of each micrograph in Figure 6.

We were trying to find out the dedoping effects by ammonium water on the morphologies of various PANINTs because we have hollow nanotubes for neat PANINTs which have higher MW and solid nanowires for low MW PANINT-pPDAs. Surprisingly, the bigger, hollow nanotubes contracted into small, solid nanowires with diameter shrunk from 200 to less than 100 nm and the empty space inside disappeared, indicating the hollow space of ES type of PANINTs were maintained by complexed DBSA which can be partly removed by $NH_4OH(aq)$ as shown in Figure 7(a,b). TEM micrographs in Figure 7(c,d) clearly demonstrated how the huge, aligned PANINT nanotubes converted to randomly oriented solid, nanowires after doping. It is understood that the paralleled nanotubes were supported by interdigitized, extended DBSA side chains which could be partly removed after dedoping and the structure shrank into separated, randomly oriented nanowires.

However, the diameters almost remained unchanged and morphology was the same after dedoping for 1% PANINT-pPDA as seen in Figure 7(e,f). It indicated that the nanowires of PANINT-pPDAs are not supported by DBSA but by the crystalline structure, which are composed of zigzagged molecules and only slightly contracted in the absence of complexed DBSA. All of them lost the ordered structure after dedoping to become EB-type polyanilines and the free carrier tails in the NIR region disappeared with dedoping as seen in Figure 4.

Wide Angled X-Ray Diffraction Patterns

Neat PANINTs has the same x-ray diffraction pattern with PANINT-pPDAs, except the additional peak at around $2\theta = 3°$ as shown in Figure 8, indicating their main crystalline lattices are the same but neat PANINTs that need a longer c-axis to

accommodate the long, alkyl chains of complexed DBSA were crystallized into the so-called layered structure usually seen for a hairy rigid rod polymer with long side chains.[28,29] The layered structure contributed to the aligned rods found in the SEM and TEM micrographs in Figures 5 and 6 and the layers can be destroyed by dedoping where complexed DBSA molecules were removed.

For PANINT-pPDA-1, PANINT-pPDA-3, and PANINT-pPDA-5, their diffraction patterns are exactly the same with absent peak at smaller angle ($<5°$) for the long c-axis and demonstrated the only two significant peaks at around $2 = 20°$ and $26°$, respectively. Neat PANINTs also demonstrated these two peaks, indicating it owns similar crystalline structure with those of PANINT-pPDAs except the longer c-axis. The common crystalline structure shared by most of the polyaromatic polymers with alternating phenyl and oxygen (polyphenylene oxide) or ketone (poly ether ether ketone) or nitrogen (polyaniline) was orthorhombic lattice (Scheme 3) and the peaks were interpreted as the (110), and (200) planes, respectively, according to it. However, other peaks represent the (111) and (102) planes of orthorhombic structure were not found.

CONCLUSIONS

In this study, we demonstrated a facile approach to prepare a nanowired polyaniline by mixing some pPDA with aniline monomers in the presence of both DBSA and phosphoric mineral acid. The obtained nanowired polyaniline has a smaller MW and can self-assemble into a network of nanowires. If no pPDA was present in the mixture, the obtained polyanilines (neat PANINTs) were nanotubular with hollow, internal core after washing by organic solvents and aligned in parallel with each to become a layered structure which can be destroyed by dedoping with ammonium water.

Another feature of the nanowired polyanilines prepared in the presence of p-PDA was that they were shorter and solid with no empty space inside even after washing by solvents, which were used to remove the noncomplexed, free DBSAs. Besides, the length of conjugation along the backbones of polyanilines decreased with pPDA due to the decreasing MW. The low MW polyanilines cannot adopt a coiled conformation to sustain the hollow, nanotubular structure like that of neat PANINTs but became zigzagged molecules packed in a nanowire.

ACKNOWLEDGMENTS

REFERENCES

1. Wu, C. G.; Bein, T. *Stud. Surf. Sci. Catal.* **1994,** *84*, 2269.

2. Misoska, V.; Price, W.; Ralph, S.; Wallace, G. *Synth. Met.* **2001,** *121*, 1501.

3. Cepak, V. M.; Martin, C. R. *Chem. Mater.* **1999,** *11*, 1363.

4. Jang, J.; Bae, J. *Adv. Funct. Mater.* **2005,** *15*, 1877.

5. Simmons, M. R.; Chaloner, P. A.; Armes, S. P. *Langmuir* **1995,** *11*, 4222.

6. Lee, Y. L.; Shin, J. I.; Park, K. W.; Holze, C. E. R. *J. Appl. Polym. Sci.* **2003,** *88*, 1550.

7. Kinlen, P. J.; Liu, J.; Ding, Y.; Graham, C. R.; Remsen, E. E. *Macromolecules* **1998,** *31*, 1735.

8. Wei, Z. X.; Zhang, Z. M.; Wan, M. X. *Langmuir* **2002,** *18*, 917.

9. Wei, Z. X.; Wan, M. X. *J. Appl. Polym. Sci.* **2003,** *87*, 1297.

10. Langer, J. J.; Framski, G.; Joachimiak, R. *Synth. Met.* **2001,** *121*, 1281.

11. Qiu, H. J.; Wan, M. X.; Matthews, B.; Dai, L. M. *Macromolecules* **2001,** *34*, 675.

12. Hsieh, B. Z.; Chuang, H. Y.; Chao, L.; Li, Y. J.; Huang, Y. J.; Tseng, P. H.; Hsieh, T. H.; Ho, K. S. *Polymer* **2008,** *49*, 4218.

13. Ho, K. S.; Han, Y. K.; Tuan, Y. T.; Huang, Y. J.; Wang, Y. Z.; Ho, T. H.; Hsieh, T. H.; Lin, J. J.; Lin, S. C. *Synth. Met.* **2009,** *159*, 1202.

14. Wei, Y.; Yang, C.; Ding, T. *Tetrahedron Lett.* **1996,** *37*, 731.

15. Shacklette, L.; Wolf, J.; Gould, S.; Baughman, R. *J. Chem. Phys.* **1988,** *88*, 3955.

16. Wei, Y.; Yang, C.; Wei, G.; Feng, G. *Synth. Met.* **1997,** *84*, 289.

17. Cao, Y.; Li, S.; Xue, Z.; Guo, D. *Synth. Met.* **1986,** *16*, 305.

18. Conwell, E.; Duke, C.; Paton, A.; Jeyadev, S. *J. Chem. Phys.* **1988,** *88*, 3331.

19. Lu, F.; Wudl, F.; Nowak, M.; Heeger, A. *J. Am. Chem. Soc.* **1986,** *108*, 8311.

20. Wei, Y.; Yang, C.; Ding, T.; Yeh, J.; Wei, G. *Polym. Mater. Sci. Eng.* **1996,** *74*, 209.

21. Lokshin, N. A.; Pyshkina, O. A.; Golubev, V. B.; Sergeyev, V. G.; Zezin, A. B.; Kabanov, V. A.; Levon, K.; Piankijsakul, S. *Macromolecules* **2001,** *34*, 5480.

22. Solomon, O. F.; Cuita, I. Z. *J. Appl. Polym. Sci.* **1962,** *24*, 683.

23. Narendra, P.; Chauhan, S.; Ameta, R.; Ameta, R.; Ameta, S. C. *J. Ind. Council Chem.* **2010,** *27*, 128.

24. Yin, H. J.; Yang, J. P. *Mater. Lett.* **2011,** *65*, 850.

25. Shen, S. Y.; Wu, Y. J.; Ho, K. S.; Hsieh, T. H.; Ho, T. H.; Wang, Y. Z.; Tseng, P. H.; Hsu, Y. C. *Polymer* **2011,** *52*, 2609.

26. Wang, Y. Z.; Hsu, Y. C.; Wu, R. R.; Kao, H. M. *Synth. Met.* **2003,** *132*, 151.

27. Ciric-Marjanovic, G.; Marjanovic, B.; Bober, P.; Rozlivkova, Z.; Stejskal, J.; Trchova, M.; Prokes, J. *J. Polym. Sci. Part A: Polym. Chem.* **2011,** *49*, 3387.

28. Zheng, W. Y.; Wang, R. H.; Levon, K.; Rong, Z. Y.; Taka, T. Pan, W. *Makromol. Chem. Phys.* **1995,** *196*, 2443.

29. Tiitu, M.; Volk, N.; Torkkeli, M.; Serimaa, R.; ten Brinke, G.; Ikkala, O. *Macromolecules* **2004,** *37*, 7364.